

A new measurement of muon spectra in the atmosphere

P. Hansen, M. Ambriola, S. Bartalucci, R. Bellotti, D. Bergström, M. Boezio, V. Bonvicini, U. Bravar, F. Cafagna, P. Carlson, M. Casolino, F. Ciacio, M. Circella, C. N. De Marzo, M. P. De Pascale, N. Finetti, T. Francke, M. Hof, J. Kremer, W. Menn, J. W. Mitchell, E. Mocchiutti, A. Morselli, J. F. Ormes, P. Papini, S. Piccardi, P. Picozza, M. Ricci, P. Schiavon, M. Simon, R. Sparvoli, P. Spillantini, S. A. Stephens, S. J. Stochaj, R. E. Streitmatter, M. Suffert, A. Vacchi, E. Vannuccini, and N. Zampa

Royal Institute of Technology, Stockholm, Sweden

University of Bari and Sezione INFN di Bari, Bari, Italy

INFN – Laboratori Nazionali di Frascati, Frascati, Italy

University of Roma “Tor Vergata” and Sezione INFN di Roma II, Rome, Italy

University of Trieste and Sezione INFN di Trieste, Trieste, Italy

R. L. Golden Particle Astrophysics Lab, New Mexico State University, Las Cruces, NM, USA

University of Siegen, Siegen, Germany

NASA/Goddard Space Flight Center, Greenbelt, MD, USA

University of Firenze and Sezione INFN di Firenze, Florence, Italy

Centre des Recherches Nucléaires, Strasbourg, France

Abstract.

We report on new measurements of the μ^+ and μ^- spectra at several atmospheric depths in the momentum range 0.3-20 GeV/c. The data were collected by the balloon-borne experiment CAPRICE98 during the ascent of the payload on the 28 May 1998 from Fort Sumner, New Mexico, USA. The experiment used the NMSU-WIZARD/CAPRICE98 balloon-borne magnet spectrometer equipped with a gas Ring Imaging Cherenkov detector and a silicon-tungsten calorimeter. This is the first time that the μ^+ component has been measured over a wide momentum range.

1 Introduction

The flux of atmospheric muons is currently of particular large interest because of the study of atmospheric neutrinos and the claim for neutrino oscillations made in 1998 by the Superkamiokande collaboration (Fukuda, et al., 1998). A measurement of the muon flux is an indirect measure of the neutrino flux and can therefore be used to improve the calculation of the atmospheric neutrino flux which in turn is used to compare with the observed neutrino rates in underground detectors like Superkamiokande.

Correspondence to: P. Hansen (hansen@particle.kth.se)

2 The experiment

The experiment was launched from Ft. Sumner, New Mexico, USA on the 28th of May 1998. The flight had a duration of 24 hours with more than 20 hours above 35 km. At this altitude, which corresponds to approximately 5.5 g/cm² of residual atmosphere above the experiment, the spectrometer collected data from more than 5.3 million cosmic ray events.

The CAPRICE98 apparatus (Ambriola, et al., 1999), from top to bottom, consisted of a gas-RICH detector, a time-of-flight (TOF) device, a magnet spectrometer, and a silicon-tungsten imaging calorimeter. The RICH detector (Francke, et al., 1999) consisted of a 1m tall gas radiator filled with high purity C_4F_{10} gas, with an average threshold Lorentz factor of about 19 at float, corresponding to a muon momentum of about 2 GeV/c. The Cherenkov light was reflected by a spherical mirror, located at the bottom of the vessel, onto a photosensitive multiwire proportional chamber with a gas read out to detect the Cherenkov light image and hence measure the velocity of the particles.

The TOF was composed of two planes, each made of two 25×50 cm² paddles of plastic scintillator, placed just above and below the tracking system and separated by 1.2 m. The TOF system was used for the trigger and to measure the time-of-flight and ionization (dE/dx) losses of the particles.

The magnet spectrometer had a superconducting magnet and a tracking device. The tracking device consisted of three

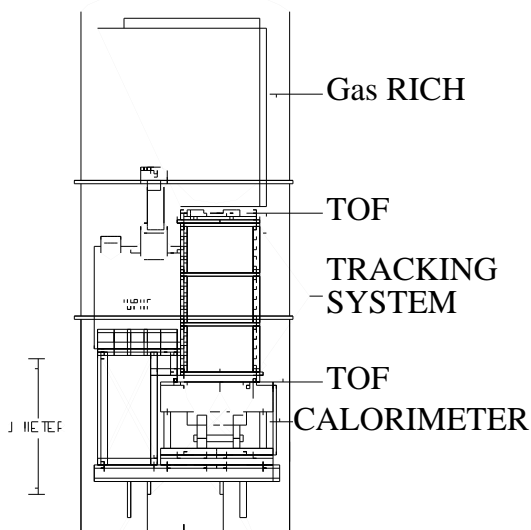


Fig. 1. The Caprice98 payload

sets of drift chambers (Hof, et al., 1994) providing a total of 18 position measurement in the direction of maximum bending, x-direction, and 12 along the perpendicular view, y-direction.

The silicon-tungsten calorimeter (Boccolini, et al., 1996; Ricci, et al., 1999) consisted of eight planes of silicon detectors interleaved with tungsten absorbers that are one radiation length thick. Each silicon plane had two layers of sensors providing x and y readouts. The vertical segmentation of the calorimeter and the use of silicon strip detectors provided information on the longitudinal and lateral profiles of the interaction along with a measure of the deposited energy. The calorimeter thickness corresponded to about 0.3 hadronic interaction lengths.

This instrument identified the nature of the particle, and measured its charge and rigidity. The unique feature of this instrument is the combination of a sensitive RICH detector and an electromagnetic calorimeter with a superconducting magnet. These independent detectors allow accurate determinations of detector efficiencies and contaminations.

It is important to stress that the major difference from the 1994 flight was that the solid radiator RICH was changed to a 1 m long gas RICH with a proton threshold of 18 GeV/c in the flights of 1997 and 1998. The CAPRICE94 spectrometer was able to identify positive muons up to 2 GeV/c. The gas RICH radiator of CAPRICE98 made it possible to safely identify μ^+ up to 20 GeV/c.

3 The selection

The CAPRICE98 instrument was well suited to measure the muon spectra and charge ratio in the atmosphere against a background of electron, protons and heavier particles. The background in the muon sample depended strongly on the atmospheric depth. At float the dominant background for pos-

itive muons was protons. For increasing atmospheric depths, the abundance of the proton component decreased becoming a few percent of the positive muon component at ground level.

Because of this varying background different selection criteria were used for muon data to maximize the efficiency while keeping the rejecting power for background events at an appropriate level.

3.1 Tracking

The tracking information was used to determine the rigidity of the particle. The trajectory was determined by fitting the information from the drift chambers. To achieve a reliable estimation of the rigidity, a set of conditions were imposed on the fitted tracks:

At least 10 (out of the 18) position measurements in the x direction and 6 (out of the 12) in the y direction were used in the fit.

There should be an acceptable chi-square for the fitted track in both directions with stronger requirements on the x-direction.

3.2 Scintillators and time-of-flight

The ionization (dE/dx) loss in the TOF scintillators was used to select minimum ionizing singly charged particles by requiring a measured (dE/dx) of less than 1.8 times the most probable energy loss by a minimum ionizing particle (mip).

Multiple track events were also rejected by requiring that not more than one of the two top scintillators's paddles was hit. The same requirement was applied to the bottom scintillators to assure a reliable TOF information.

With the TOF information we can estimate the particle velocity (β) and by requiring $\beta \geq 0$ we can select downward moving particles that assured that no contamination of albedo particles remained in the selected sample.

The velocity β of the particle from the TOF was compared to the β obtained from the fitted deflection assuming that the particle had the mass of a muon. The difference was required to be within one standard deviation.

3.3 The RICH

The RICH was used to measure the Cherenkov angle of the particle and thereby its velocity. Muons started to produce Cherenkov photons in the C_4F_{10} gas at about 2 GV and protons at about 18 GV while electrons were above threshold in the whole rigidity range of interest. Hence, below 2.1 GV muons were selected requiring no light while above 2 GV muons were selected according to their reconstructed Cherenkov angle. Between 2 and 2.1 GV, events were selected as muon if they did not produce a Cherenkov signal or if the reconstructed Cherenkov angles were consistent with that of muons with the measured rigidity. In this way, we took into account both the Poisson fluctuations in the number of photoelectrons and the variation of the threshold due to pressure

changes. The Cherenkov angle was reconstructed from the geometrical distribution of the signals in the pad plane. The quality of the measured Cherenkov angle depends on the number of pads used in the fit. Therefore, we required that the number of pads with signal from Cherenkov light was greater than 10. Finally, we required that the measured Cherenkov angle agreed within three standard deviation of the resolution from the expected Cherenkov angle for a muon.

The RICH was also used to reject events with multiple charged particles. Since ionization from charged particles produced significantly higher signals than converting Cherenkov photons, we required that an event contained only one cluster of pads with high signal.

3.4 The calorimeter

The calorimeter was used to separate non-interacting particles from showers. It was very powerful to reject electrons or interacting hadrons but it could not distinguish muons from non-interacting pions or protons except at low momenta where the particles could be separated using their energy losses in the silicon detectors.

4 Contamination

We estimated the contamination of protons in the muon sample with the data at float. We used the data at float because in that way it was easy to select a clean and large sample of protons. Below 1.5 GV the TOF system was efficient in rejecting protons and the RICH started to reject them above 2.1 GV. The overall proton rejection factor was better than 10^3 and, hence, proton contamination was essentially negligible in all momentum intervals of this analysis with the exception of 1.5 to 2.1 GeV/c where μ^+ could not be separated from protons. Therefore, no results on μ^+ are presented in this momentum interval.

Electrons were efficiently rejected by the calorimeter in the whole rigidity range and by the RICH below about 5 GV, hence the remaining electron contamination was negligible.

5 Efficiency determination

In order to accurately determine the fluxes of the various types of particles, the efficiency of each detector was carefully studied using ground, ascent and flight data. To determine the efficiency of a given detector, a data set of muons was selected by the remaining detectors. The number of muons correctly identified by the detector under test divided by the number of events in the data set provided a measure of the efficiency. This procedure was repeated for each detector. The efficiency of each detector was determined as a function of rigidity in a number of discrete bins and then parameterized to allow an interpolation between bins.

For the efficiency study, a large sample of negative muons collected at ground prior the flight was used. Then, the re-

sults were cross-checked with smaller samples of negative muons from flight data.

5.1 TOF efficiency

The (dE/dx) and β selection were studied using the negative muons selected by the calorimeter and the RICH. The efficiency was found to be 0.86 for lower momenta, decreasing to 0.8 for higher momentum.

5.2 Calorimeter efficiency

The calorimeter efficiency was determined by selecting a sample of muons with the TOF and the RICH and cross-checked with Monte Carlo simulation. The efficiency was found to be constant at about 92% in the whole rigidity range.

5.3 RICH efficiency

The RICH selection efficiency was obtained selecting muons with the calorimeter and TOF system. Below the muon RICH threshold, the selection efficiency was found to be constant at about 94%. At the threshold (2 GV) it dropped to about 30% and then it increased and reached a constant value of about 74% above 3 GV.

6 The flux of muons

The absolute particle fluxes were calculated from the number of observed muons taking into account the spectrometer geometrical factor and live time as well as selection efficiencies. The Figures 2 and 3 show the muon flux as function of the momentum for positive and negative muons at five different atmospheric depth. Here we only present some intervals for clarity reasons. The statistical errors are small and not visible in the data points. The data are compared with data of CAPRICE94 (Boezio, et al., 2000) and in the case of negative muons also with MASS89 (Bellotti, et al., 1996) and MASS91 (Codino, et al., 1997). For MASS89 and MASS91 we used the half of the interval like the centre of gravity of the rigidity.

7 Conclusion

We present new experimental data on atmospheric muons that show a good agreement with the data of CAPRICE94, MASS89 and MASS91. It is important to stress that this is the first time that the atmospheric positive muons were measured at rigidities up to 20 GV in a balloon-borne experiment. It was possible because the CAPRICE98 apparatus used a gas RICH detector with an average threshold Lorentz factor of about 19 at float (corresponding to a muon momentum of about 2 GeV/c). The data will allow a detail comparison with results of atmospheric shower simulation.

For negative muons the CAPRICE98 data are in good agreement with the CAPRICE94 data and also with the MASS data sets, showing an approximate exponential decrease as a

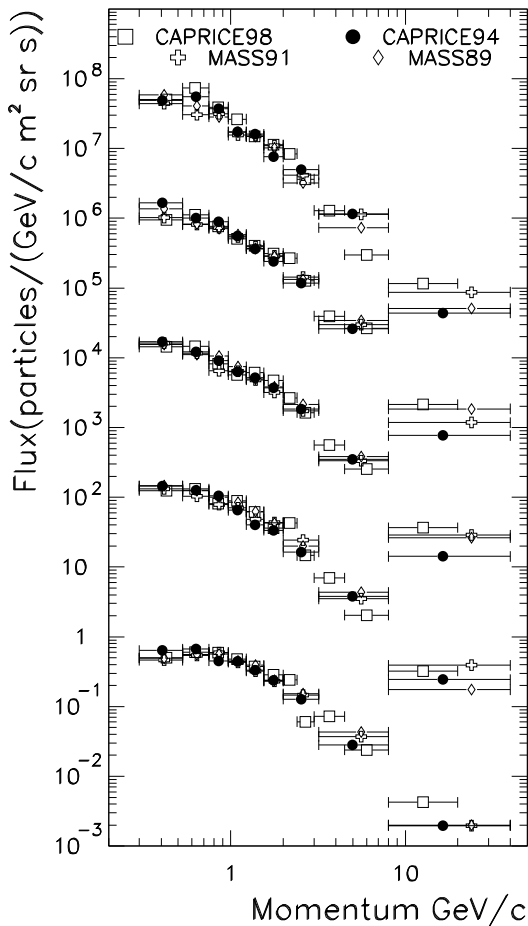


Fig. 2. Negative muon spectra for several atmospheric depth intervals. From top to bottom are the atmospheric ranges in g/cm^2 : 15-35 (scaled by 10^{10}), 65-90 (10^8), 120-150 (10^6), 190-250 (10^4), 380-580 (10^2)

function of momentum above 1 GeV/c. For positive muons there is a good agreement between the CAPRICE data from 1998 and 1994 for muon momenta below 2 GeV/c. Below 1 GeV/c, the CAPRICE98 results are lower than the results from CAPRICE94 which could indicate geomagnetic effects (the solar activity was similar for the two experiments). For momenta above 2 GeV/c the CAPRICE98 follows an approximate exponential decrease as a function of momentum, similar to the negative muon data.

References

Ambriola, et al.(1999) Nucl. Phys. B (Proc. Suppl),78, 32
 Bellotti, et al.(1996) Phys. Rev. D 53, 35 (1996)

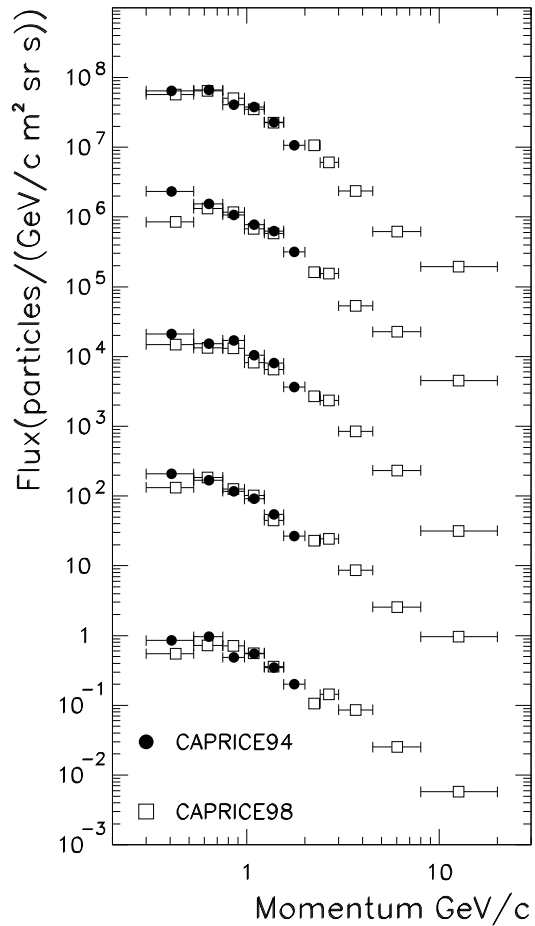


Fig. 3. Positive muon spectra for several atmospheric depth intervals. From top to bottom are the atmospheric ranges in g/cm^2 : 15-35 (scaled by 10^{10}), 65-90 (10^8), 120-150 (10^6), 190-250 (10^4), 380-580 (10^2)

Bocciolini, et al.(1996) Nucl. Instrum. Methods Phys. Res. A370, 403
 Boezio et al.(1999) Astrophys. Journ. 518, 457
 Boezio et al.(2000) Phys Rev D62,032007
 Codino, et al.(1997) J. Phys. G: Nucl. Part. Phys. 23, 1751 (1997)
 Francke, et al.(1999) Nucl. Instrum. Methods Phys. Res., A433,87
 Fukuda, et al.(1998) Phys. Rev. Lett. 81. 1562
 Hof, et al.(1994) Nucl. Instrum. Methods Phys. Res.,A345,561
 Ricci, et al.(1999) Proc. 26th Int. Cosmic-Ray Conf. (Salt Lake City),5, 49